EXPERIMENTS ON LASER AND MICROWAVE PROBING OF PLASMA, AND MEASUREMENTS OF THE DIAMAGNETIC EFFECT ON THE TOKAMAK T-3a INSTALLATION

A. M. ANASHIN, E. P. GORBUNOV, D. P. IVANOV, S. E. LYSENKO, N. J. PEACOCK,[1] D. C. ROBINSON,[1] V. V. SANNIKOV, and V. S. STRELKOV

Submitted December 23, 1970

Zh. Eksp. Teor. Fiz. 60, 2092–2104 (June, 1971)

Thomson scattering and electrical, microwave, corpuscular, and diamagnetic measurements have been used to determine the electron temperature of plasma in the Tokomak T-3a installation. The experiments were confined to the plasma density range 10^{13}–4×10^{13} cm^{-3}, discharge currents of 40–130 kA, and stabilizing magnetic fields of 17–38 kOe. It is shown that most of the plasma electrons have a near-Maxwellian energy distribution with a temperature between 0.5 and 2 keV. The temperature reaches steady-state values during the time of the process (35 msec). The plasma density obtained from measurements of the absolute intensity of scattered laser radiation is close to that measured with the microwave interferometer. The radial distributions of temperature, electron density, and electron pressure at various stages of the discharge have been determined. There is good agreement between the density distributions measured with the aid of the laser and with the multichannel microwave interferometer. The transverse energy of the plasma deduced from magnetic measurements is in satisfactory agreement with that calculated from laser, microwave, and corpuscular measurements. The electron temperature increases with increasing current and decreasing density, but is practically independent of the stabilizing field. The value of $B_J = 8\pi\bar{p}/H_J^2$ at the time of maximum stored energy in the plasma lies in the range 0.4 ± 0.1, and exceeds unity at the end of the process. Both the transverse electron temperature distribution and the energy balance in the electron component of the plasma can be explained by the anomalous electron thermal conductivity. The particle lifetime in the plasma calculated from the measured H_α intensity is at least several times greater than the energy containment time. The degree of anomaly of the plasma resistance increases rapidly with increasing ratio of the drift velocity to the ion sound velocity.

INTRODUCTION

DETERMINATIONS of the transverse energy of plasma from the diamagnetic effect have been used to determine the mean electron temperature during thermal-insulation and plasma-heating studies on toroidal installations in the Tokomak series. The plasma density was known from microwave measurements, and the contribution of the ion component could be calculated by analyzing the neutral-atom spectrum emitted by the plasma column. The electron temperature deduced from magnetic measurements was found to be several times greater than that found from the electrical conductivity of plasma. The high electron temperatures (up to 1 keV) at sufficiently long energy containment times (up to 10 msec) were reported in[1] to lead to the conclusion that there is a substantial difference between the energy and the Bohm containment time.

The validity of this fundamental conclusion is, however, doubtful because the electron temperature is deduced from the transverse energy of the plasma. It is therefore desirable to find a direct method of measuring the electron temperature. This was done on the Tokomak T-3a installation by analyzing the spectrum of the laser radiation scattered by the plasma.[2] Apart from the electron energy distribution, the method could be used to find the electron density and the radial distribution of these parameters. The use of the laser method in conjunction with other data provides sufficient information for an independent determination of the transverse energy of the plasma. This provides information about the reliability of diamagnetic measurements and their interpretation.

1. EXPERIMENTAL METHOD

1. The electron temperature T_{el} was determined from the spectrum of the scattered laser radiation.[2] We used a ruby laser producing giant pulses with radiation energy of about 5 J and pulse length of 20–30 nsec. Light scattered at right-angles to the incident beam was intercepted by the entrance slit of a high-luminosity spectrograph with a ten-channel photoelectric detector. A special periscopic system at the entrance to the spectroscopic equipment enabled us to record the light scattered from different points along the diameter of the plasma column so that the radial distribution of the electron temperature and density could be established. Since the Debye length under our experimental conditions was much greater than the laser wavelength, the scattering parameter was $\alpha \ll 1$.[13] The spectrum of the scattered radiation then reflected the velocity distribution of the electron component of the plasma. When the velocity distribution was Maxwellian, the scattered spectrum was Gaussian with a half-width proportional to the square root of the temperature.

2. The ion temperature was determined by analyz-

[1] Culham Laboratory, Great Britain.

ing the neutral-atom spectrum emitted by the plasma.[4] It was shown in[5] that this method yielded the ion temperature in the central regions of the plasma.

3. The electron density n and its radial distribution n(r) were determined by multichord phase exploration of the plasma using 2-mm waves.[6,7] Similar experiments were used earlier to show that the electron density in the T-3a installation was symmetric with respect to the equatorial plane, and the lines of equal density were, in fact, circles. In the present research, the microwave exploration of the plasma was carried out along seven vertical chords. For each of these chords we recorded the time dependence of the microwave phase shift, and then by solving the integral Abel equations we were able to construct the density profile for any particular instant of time. Local values of the electron density were determined from absolute measurements of the incident and scattered laser fluxes. As noted in[2], there is good agreement between the time dependence and the radial density distribution found by the two methods.

4. The transverse energy of the plasma was determined by measuring the change in the longitudinal magnetic flux.[8] In contrast to the T-3 installation, the coils mounted on the T-3a had shorted metal bodies. Because of this, the procedure of the diamagnetic measurements which we have used differed from that described in[8] by the presence of special coils distributed uniformly over the toroidal chamber. The method used to suppress the high-frequency pulses of the magnetic field, and the use of correction circuits which eliminated the effect of currents in the shorted bodies of the main coil, are described. The attendant complication of the apparatus, and the smaller difference between the discharge pulse length and the stabilizing field pulse have led to a lower accuracy as compared with[8]. In our experiments this did not exceed 30%.

5. We have also carried out the usual measurements of the discharge current, the displacement of the current relative to the center of the chamber (using magnetic probes[9]), and the vertical, transverse, and longitudinal magnetic fields.

The diamagnetic, microwave, and electrical data were then analyzed on a computer, and yielded the time dependence of the displacement of the plasma column, its total inductance, its electrical conductivity per unit length σ_r, the amount of Joule heating in the plasma, and the energy lifetime τ_E.[10] When the corresponding set of equations was solved, we allowed for the effect of the finite electrical conductivity of the copper envelope on the equilibrium of the plasma column.[11] We were able to find from the calculated total inductance the internal inductance as a function of time, having taken the radius of the aperture in the diaphragm $a_0 = 17$ cm as the radius of the current.

2. RESULTS

Figure 1 shows a typical spectrum of the scattered signal. The points show the relative intensities within each measuring channel, using a 78-Å channel width. The experimental points are in satisfactory agreement

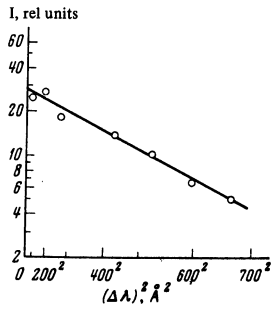

FIG. 1

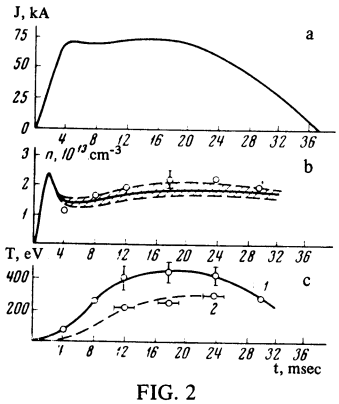

FIG. 2

FIG. 1. Intensity of scattered light as a function of the square of the wavelength difference. Straight line corresponds to $T_{el} = 640$ eV.

FIG. 2. Electron density and temperature on the axis of the plasma column as a function of time during the discharge. a) Discharge current oscillogram; b) density obtained by analyzing microwave data (solid line) and laser measurements (points). Shaded region shows the spread in density values from discharge to discharge; c) electron temperature $T_{el}(0)$ from the laser experiment (curve 1) and the ion temperature T_i (curve 2).

with the linear relationship between the logarithm of the intensity and the square of the wavelength difference, and this indicates that the electron velocity distribution is Maxwellian. The measurements were carried out simultaneously in all the channels for each laser pulse, but in order to reduce the experimental uncertainties the spectrum was constructed for 5—10 plasma discharges with the same initial conditions. The uncertainty in the measured temperature was 5—15% for most of our results. For the limiting temperatures (>100 eV and >1.5 keV) the uncertainty did not exceed 20%.

Comparison of microwave and laser measurements of the electron density n (Fig. 2) leads to the conclusion that the temperature found from the width of the scattered light spectrum can be ascribed to the main mass of electrons in the plasma to within the experimental error. It is clear that the electron temperature reaches steady values after about one-third of the duration of the discharge. Figure 2 also shows the ion temperature as a function of time.

The observed agreement between the radial density distributions obtained with the multichannel radio interferometer in the case of vertical measurements, and from the intensity of scattered light for horizontal observations[2], confirms the earlier conclusion[6] that the density distribution is axially symmetric during the initial and intermediate discharge stages. The temperature distribution is probably also axially symmetric during these stages. Special experiments have shown that the temperature distribution is symmetric when the point of observation is moved up and down relative to the axis of the column. All this enables us to interpret temperature variation determined from scattered-light measurements at different heights above the equatorial plane as the radial distribution of the plasma temperature.

Figure 3 shows the electron temperature and plasma density and pressure over the cross section of the

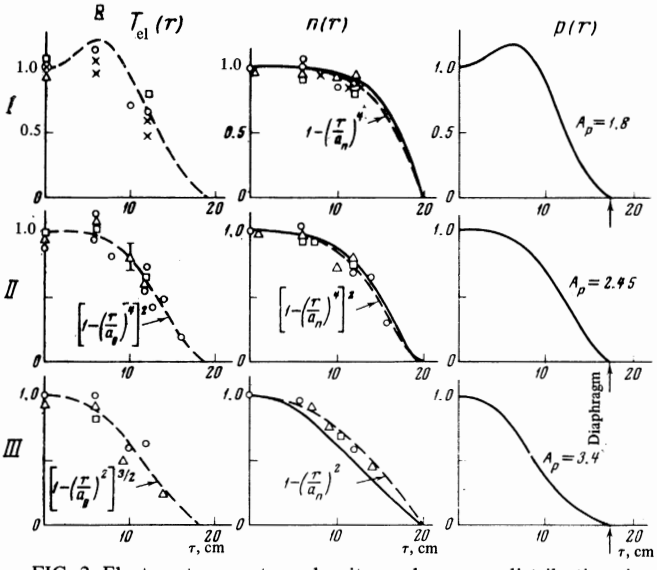

FIG. 3. Electron temperature, density, and pressure distributions in relative units using different discharge stages: I–t = 4 msec; II–t = 16 msec; III–t = 30 msec. The points were obtained from laser measurements. Broken curves are approximate (a_n = 20 cm, a_0 = 17 cm). Solid curves representing n(r) were obtained from microwave data.

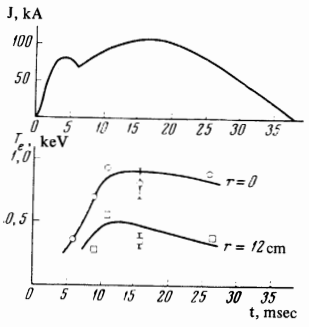

FIG. 4.

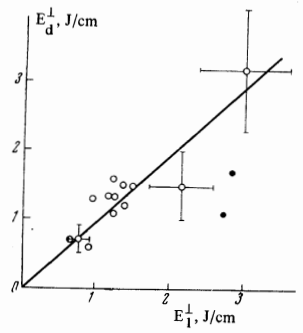

FIG. 5.

FIG. 4. Repeated current rise. Upper figure–discharge current; lower figure–temperature at the center and at a radial distance of 12 cm.

FIG. 5. Transverse energy during the intermediate stage of the discharge determined from diamagnetic measurements ($E_d^\perp$) and calculated from $T_{el}(r)$, $T_i(r)$, and $n(r)(E_I^\perp)$. Full points correspond to the appearance of weak instability.

plasma column. The different shape of $T_{el}(r)$ and $n(r)$ curves for different discharge conditions is unimportant (the broken curves are based on formulas indicated in the figure). At the beginning of the discharge the temperature at the edge of the plasma column is somewhat higher than at the center, which is probably due to the skin effect. The plasma density distribution is flatter than a quadratic parabola. During the intermediate discharge stage the electron temperature and density distribution can be approximately represented by the function $[1 - (r/a)^4]^2$, where a is the distribution parameter which is equal to the radius a_n of the chamber in the case of $n(r)$, and to the radius a_0 of the diaphragm in the case of $T_{el}(r)$. At the end of the discharge the radial temperature and density distributions become sharper. The pressure distribution of the electron component in the radial direction was obtained as a product of the $T_{el}(r)$ and $n(r)$ curves. To calculate the plasma energy we shall use the mean plasma pressure which we shall calculate from the maximum values of $n(0)$ and $T(0)$ and the coefficient A_p which characterizes the form of the radial pressure distribution

$$\bar{p} = \overline{nT} = n(0)T(0)/A_p.$$

The values of A_p are shown in Fig. 3.

We must note one further experimental result, concerned with the radial temperature distribution measured by the laser method. In special experiments with a repeated current rise (Fig. 4) one would expect a more clearly defined temperature skin effect which is not clearly seen during the initial rise of the current (Fig. 3). Laser measurements of the temperature at two points along the radius of the plasma column did not, however, reveal this effect.

The above data on the temperature and density distributions over the cross section of the plasma column can be used to determine the transverse energy component for the electrons per unit length of the plasma column. If we use the measured values of the ion temperature, and if we assume that this temperature is distributed over the cross section in the same way as for the electron component, while the impurity density is low so that $\gamma = n_i/n_e \approx 1$, the total transverse energy stored in the plasma can be calculated from the formula

$$E^\perp = 2\pi \int_0^a n(r)\,[T_e(r) + \gamma T_i(r)]\,r\,dr.$$

This same quantity can be found directly by another independent method, namely, by diamagnetic measurements.

Figure 5 shows the energy stored in the plasma, obtained by different methods. The points represent values of $E_I^\perp$ and $E_d^\perp$ averaged over a number of pulses for different discharge conditions at maximum plasma energy (15–20 msec). The accuracy of the diamagnetic method, in this case, is about 30%, whilst the calculated $E_I^\perp$ deduced from laser and interferometric data are good to 20%. Figure 5 indicates all the experimental conditions under which the diamagnetism and laser scattering were simultaneously investigated. When the radial temperature and density distributions were not recorded, we used a function of the form $[1 - (r/a)^4]^2$ to calculate the transverse energy. When the ion temperature necessary to compare $E_I^\perp$ and $E_d^\perp$ was not measured, it had to be calculated from the empirical formula given in[12]. Figure 5 shows that the values of $E^\perp$ determined by different methods are in agreement to within experimental error in a broad range of discharge parameters. The exceptions are provided by those conditions under which magnetohydrodynamic instabilities are observed (full points in Fig. 5).

Figure 6 shows the main parameters as functions of time during the discharge. The radial density distribution $n(r)$ obtained by the microwave method was used to determine the maximum electron density n_0 at the center, its mean $\bar{n}$ over the diameters, and the total number N of particles within the cross section of the plasma column. During the initial discharge stage the

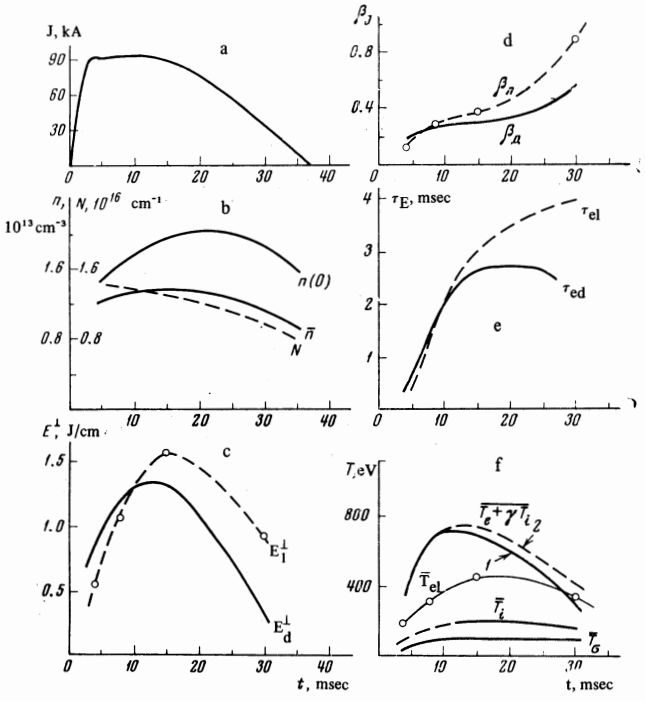

FIG. 6. Plasma parameters as functions of time (H = 25 kOe). a–Discharge current; b–electron density n(0) on the axis of the plasma column. The electron density averaged over a diameter, $\bar{n}$, and the total number N of electrons per unit length of the plasma column deduced from multichord microwave measurements; c–transverse plasma energy determined from laser and diamagnetic data; d–comparison of the values of β_J deduced from diamagnetic measurements and calculated from $T_{el}(r)$, $T_i(r)$, and n(r); e–energy lifetime calculated from diamagnetic and laser data; f–temperature averaged over the cross section: $\overline{T}_{el}$–laser data, $\overline{T}_i$–analysis of atomic spectra, $\overline{T}_\sigma$–calculations based on the electrical conductivity, $\overline{T_e + \gamma T_i}$–from diamagnetic measurements.

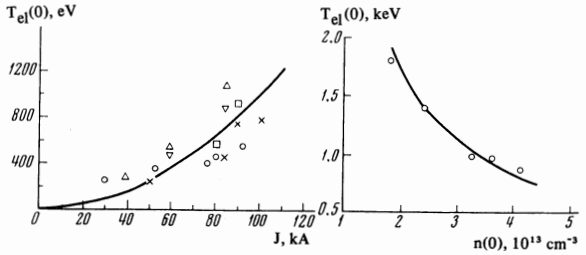

FIG. 7 FIG. 8

FIG. 7. Electron temperature as a function of the discharge current under different conditions for t = 25 msec:

	n(0), 10^{13} cm^{-3}	H, kOe
○	2 – 3	25
△	1,5	17
□	2	25
▽	1,5	25
×	2	25

Solid curve represents quadratic dependence of the current.

FIG. 8. Electron temperature as a function of electron density on the axis (H = 35 kOe, J = 130 kA, t = 20 msec).

distribution n(r) is almost uniform up to three-quarters of the radius of the chamber. The mean density $\bar{n}$ is only slightly lower than the maximum density n(0). The n(r) distribution becomes sharper during the discharge, and n(0) continues to grow for about 20 msec, while the total number of particles within the cross section of the plasma column decreases with a decay time of the order of 85 msec.

It is clear from Fig. 6c that the time dependence of the energy determined by the laser and diamagnetic methods is in adequate agreement with the exception of the final stage of the discharge. The difference found during this final stage is connected with a systematic error during the analysis of the diamagnetic data which increases toward the end of the current pulse so that the values of the transverse energy deduced from laser data are more reliable toward the end of the process.

The time dependence of the quantity $\beta_J = 8\pi\bar{p}/H_J^2$, shown in Fig. 6d, has an analogous shape. At the end of the pulse the value of β_J, found from the laser data, reaches a figure of the order of unity.

The energy containment time τ_E found from the corresponding values of the transverse energy $E_I^\perp$ and $E_d^\perp$ are shown in Fig. 6e.

The mean temperature $\overline{T_e + \gamma T_i}$ was calculated in[13] from measurements of the diamagnetic effect, assuming parabolic plasma density and temperature distributions along the radial direction. Curve 1 in Fig. 6f was obtained by this method. Curve 2 was calculated with allowance for the measured radial plasma density distribution. It is clear from the figure that this correction is quite small. The values of the electron temperature $\overline{T}_{el}$ given in the figure were obtained by averaging over the cross section, taking into account the radial distribution $T_{el}(r)$ measured by examining the Thomson scattering. The quantity $\overline{T}_\sigma$ was calculated from the electrical conductivity on the assumption of a parabolic temperature distribution, and the relationship between the electrical conductivity and temperature was specified by the Spitzer formula.

Thus, both the absolute values and the time dependence of the various plasma parameters determined from the laser measurements are in satisfactory agreement with the results of calculations based on data obtained by the diamagnetic method.

The dependence of the temperature determined by the laser method on the current and density of electrons in the plasma is also analogous to that found earlier from diamagnetic measurements.[10] Figure 7 shows that $T_{el}(0)$ is roughly proportional to the square of the current. Figure 8 illustrates the reduction in the electron temperature with increasing electron density. It is clear from Fig. 9 that the energy stored in the plasma, as deduced from laser measurements, is proportional to the square of the current during the intermediate discharge stage (15–20 msec). Throughout the range of parameters which we have investigated, the value of β_J turns out to be almost constant and equal to 0.4 ± 0.1.

Comparison of the electrical conductivity σ_R per unit length of the column with σ_C calculated from the Spitzer formula for hydrogen plasma, using the measured electron temperature, provides a new confirmation of the phenomenon of anomalous plasma resistance established earlier on the basis of diamagnetic measurements.[14] The degree of anomaly is defined by

$$\eta = \frac{\sigma_C}{\sigma_R} = \frac{\sigma_0}{\sigma_R}\int_0^a T_{el}^{3/2}(r)\,r\,dr,$$

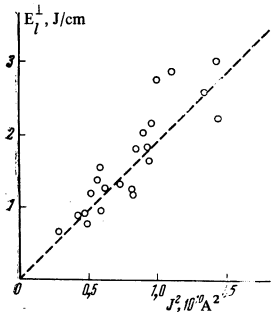

FIG. 9

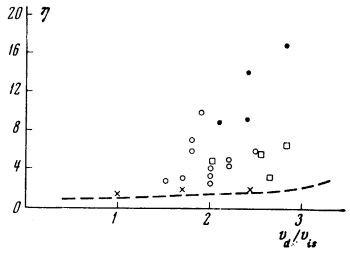

FIG. 10

FIG. 9. Transverse plasma energy as a function of the square of the current. Broken line corresponds to $\beta_J = 0.4$.

FIG. 10. Degree of anomaly of the plasma resistance η as a function of the ratio of the drift to the ion sound velocities: □–initial stage (4-12 msec), ○–intermediate stage (15-25 msec), ×–final stage (27-30 msec) (H = 25 kOe, J = 90 kA); ●–intermediate stage of discharge in the presence of weak instability (H = 36 kOe, J = 130 kA). Broken curve based on the data in [14].

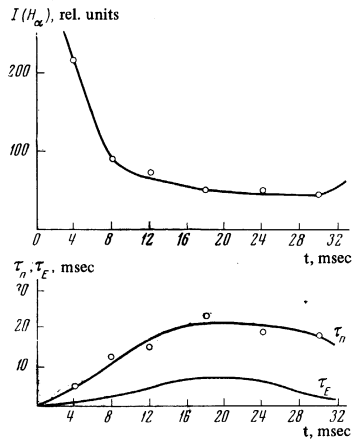

FIG. 11

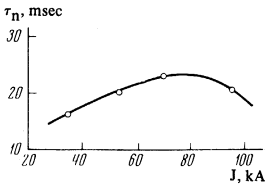

FIG. 12

FIG. 11. H_α intensity as a function of time, the particle containment time, and the energy time τ_E.

FIG. 12. τ_n as a function of the discharge current.

where σ_0 is the proportionality factor in the Spitzer formula. In contrast to[14], in our case, η already increases rapidly for $v_d/v_{is} = 1.5$ (drift velocity $v_d = J/\pi a^2 e\bar{n}$, sound velocity $v_{is} = \sqrt{2T_e/M}$, M is the ion mass). The velocity ratio does not exceed 3 even for high current densities $j \geq 200$ A/cm^2, and not very high densities $n \approx 1 \times 10^{13}$ cm^{-3}. The value of η under these conditions reaches 20. When the temperature is calculated from the resistance it is, in general, necessary to introduce a correction, taking into account the presence of trapped particles.[15] Estimates show, however, that for the geometry of the T-3a this correction does not exceed 50%. When collisions are present the correction is lower. Impurities may be a more important factor. It is important to note that the entire series of experiments which we are describing was carried out under vacuum conditions somewhat poorer than usual in the Tokomak installations. The initial pressure was no better than 3×10^{-7} Torr, and the impurity level may have been higher than earlier.[13]

In addition to temperature and density measurements, the apparatus used to record the scattered light could also be employed to determine the absolute intensity of the $H\alpha$ line. These data enabled us to estimate the density of the neutral hydrogen atoms in different regions of the plasma column and the charged-particle containment time for the plasma.[16] The change in the plasma density was connected with charged-particle losses at the diaphragm and walls of the vacuum chamber, and the arrival and subsequent ionization of neutral atoms. From the balance between the rates of loss of particles and ionization of neutral atoms in the plasma column we can obtain an expression for the charged-particle lifetime:

$$\tau_n = \frac{\bar{n}}{\mathcal{J} - d\bar{n}/dt},$$

where $\bar{n}$ (mean electron density) and $d\bar{n}/dt$ (rate of change of density) are determined by the microwave method, and $\mathcal{J}$ is the rate of ionization of neutral atoms, which can be expressed in terms of the absolute $H\alpha$ intensity $I(H\alpha)$ and the number of ionizations per photon

$$\mathcal{J} = \xi I(H_\alpha),$$

where $\xi \sim 4$ under our discharge conditions ($T_e > 100$ eV, $n \sim 1 \times 10^{13}$ cm^{-2}). Experiments have shown that the strongest radiation corresponds to an annular region in the plasma, 2–3 cm wide, at a distance of about 13 cm from the magnetic axis and, therefore, the error in the calculated $I(H\alpha)$ is quite high for the central zone. One can only speak of the upper limit for this quantity.

The absolute intensity of the $H\alpha$ line enables us to find the neutral-atom density. In the annular region at the edge of the diaphragm it amounts to 2×10^9 cm^{-3}. Near the axis of the plasma column this density is lower by a factor of at least 10. Figure 11 shows that the particle containment time τ_n, calculated from the $H\alpha$ intensity, exceeds by a substantial factor the energy lifetime τ_E of the plasma. We note that the particle lifetime refers to the boundary, where the interaction between the neutral atoms and the plasma is strongest. The particle containment time near the center of the column may be much greater.[5] As the discharge current increases, the containment time τ_n at higher currents is probably connected with the development of macroscopic instabilities which were observed at this time.

3. DISCUSSION

Comparison of the transverse plasma energy deduced from the diamagnetic effect with values calculated from the laser and microwave measurements (Fig. 5) shows good agreement during different discharge states. The only exception corresponds to high densities and high currents (full points in Fig. 5). Weak instabilities begin to develop in this case. The electron temperature at the center, $T_{el}(0)$, does not then fall rapidly, whereas the transverse energy turns out to be lower in all the cross sections than in the case of stable states. This can be explained by the develop-

ment of surface modes[17] leading to an increase in losses and to a cooling of the peripheral parts of the column. The radial distribution $T_{el}(r)$ was not recorded under these conditions, and to calculate $E_I^{\perp}$ we used the same radial temperature and density distributions as for the stable states. This may mean that the resulting values of $E_I^{\perp}$ may be too high.

Experiments on Thomson scattering show that the electron energy distribution is nearly Maxwellian. It is possible, in principle, that there is a group of electrons whose temperature lies below or above the measurement limits. However, the agreement between the density obtained with the radio interferometer and that found from Thomson scattering, and the agreement between $E_I^{\perp}$ and $E_d^{\perp}$, show that the density of fast electrons with energies greater than 100 keV cannot exceed 1% of the total plasma density. The presence of fast electrons of lower energy is not very likely because, under our conditions, the Maxwellization time of the electron component is much less than the energy containment time. In other words, even if we suppose that the entire energy liberated by the current in the plasma is transferred not to all but only to some of the electrons, the difference between the temperature of this group and that of the remaining mass of electrons cannot be large.

It is interesting to compare our data on the radial electron temperature distribution with calculations reported in[18]. This calculation involves the solution of a set of equations including local energy balance equations for ions and electrons, and the Maxwell equations for the parameters of the T-3a. The thermal conductivity is determined from the classical theory of two-body collisions for a toroidal plasma column.[19] The effective collision frequency is assumed to depend on the ratio of the electron drift velocity to the sound velocity in such a way that the total resistance of the plasma column agrees with the experimental value. The electron thermal conductivity is therefore increased as the collision frequency increases by a factor of up to 10. Comparisons show that the calculated electron temperature is somewhat higher than the measured values. Moreover, the numerical values have a greater tendency to the "skin effect" than the experimental values.

The last fact is also reflected in the absence of the temperature skin effect in the case of repeated current rise. Numerical calculations for this case were not performed, but since the conductivity reaches high values when the growing current is switched on, the skin effect should appear more clearly. This result may be a consequence of a substantial difference between the electron thermal conductivity and the classical value. Another explanation is connected with the high radiation losses of the electron component, and this seems to us more probable in view of the estimated radiation energy given in[20], where it is shown that energy losses associated with radiation and charge transfer amount to no more than 10—15% of the energy input into the plasma.

The degree of anomaly of the plasma resistance is shown in Fig. 10 as a function of the ratio of the drift velocity to the sound velocity, and may be looked upon as an indication that the ion-acoustic instability is the reason for the anomalous resistance.[21] There may be, however, other factors producing this effect, for example, an increase in the effective plasma ion charge due to impurities. The experimental data given in Fig. 10 are not inconsistent with the dependence of the degree of anomaly on v_d/v_{is} adopted in[18]. The analysis of the plasma energy balance given in[10] also indicates the important role of the anomalous electron thermal conductivity.

In the time-independent case, when the energy of the plasma column does not vary, we can readily obtain a relation between the energy time τ_E and the electrical conductivity σ_R of the plasma: $\tau_E = \text{const} \cdot \beta_J a^2 \sigma_R$. Let us now consider Fig. 9 which shows the transverse energy as a function of J^2. As can be seen, for the plasma parameters we have investigated, the quantity β_J remains almost constant and amounts to 0.4 ± 0.1, i.e., the energy lifetime τ_E is directly proportional to σ_R and hence to the effective collision frequency. The plasma energy losses may, in general, occur as a result of the following main processes: diffusion, thermal conduction, charge transfer, and radiation. Comparison of the particle lifetime with the energy lifetime (Fig. 11) shows that, in our case, the diffusion is not the main loss mechanism. Radiation and charge transfer losses are also small.[20] The main energy losses are therefore due to thermal conductivity, and the relation between τ_E and σ_R shows that this is determined by the effective collision frequency.

We note that at high densities the classical ion thermal conductivity may play an appreciable role in the energy balance of the plasma.

The present paper includes the results of a joint investigation of Thomson scattering performed in 1969 by a group from the Culham Laboratory and the staff of the I. V. Kurchatov Institute of Atomic Energy on the T-3a Tokomak installation.

The authors are indebted to Dr. R. S. Pease, Director of the Culham Laboratory, and to Academician L. A. Artsimovich, Head of the Department of Plasma Studies of the I. V. Kurchatov Institute of Atomic Energy for the organization of the joint research project, their constant interest, and discussions of results. We are also indebted to the technical staff of the Culham Laboratory for the preparation of this complex experiment in a very short time and to the servicing personnel of the T-3a installation for ensuring the continuous operation and for help in the laser, electrical, microwave, and corpuscular measurements. Special thanks are due to A. V. Glukhov, P. D. Wilcock, and M. D. Forrest.

[1] L. A. Artsimovich, G. A. Borbovskiĭ, S. V. Mirnov, K. A. Razumova, and V. S. Strelkov, At. Energ. 22, 259 (1967).

[2] N. J. Peacock, D. C. Robinson, M. J. Forrest, P. D. Wilcock, and V. V. Sannikov, Nature 224, 448 (1969).

[3] E. E. Salpeter, Phys. Rev. 120, 1528 (1960).

[4] V. V. Afrosimov and M. P. Petrov, Zh. Tekh. Fiz. 37, 1189 (1967) [Sov. Phys.-Tech. Phys. 12, 863 (1968)].

[5]L. A. Artsimovich, E. P. Gorbunov, and M. P. Petrov, ZhETF Pis. Red. 12, 89 (1970) [JETP Lett. 12, 62 (1970)].

[6]E. P. Gorbunov, Yu. N. Dnestrovskiĭ, D. P. Kostomarov, and B. F. Mul'chenko, Diagnostika plazmy (Collection: Plasma Diagnostics), Gosatomizdat, 1968, Vol. 2, p. 188.

[7]E. P. Gorbunov, Yu. N. Dnestrovskiĭ, and D. P. Kostomarov, Zh. Tekh. Fiz. 38, 812 (1968) [Sov. Phys.-Tech. Phys. 13, 609 (1969)].

[8]S. V. Mirnov, At. Énerg. 26, 458 (1968).

[9]S. V. Mirnov, At. Énerg. 17, 209 (1964).

[10]E. P. Gorbunov, S. V. Mirnov, and V. S. Strelkov, Nucl. Fusion 10, 43 (1970).

[11]A. E. Bazhanova, V. S. Strelkov, and V. D. Shafranov, At. Énerg. 20, 146 (1966).

[12]L. A. Artsimovich, A. V. Glukhov, and M. P. Petrov, ZhETF Pis. Red. 11, 449 (1970) [JETP Lett. 11, 304 (1970)].

[13]L. A. Artsimovich, G. A. Bobrovskiĭ, E. P. Gorbunov, D. P. Ivanov, V. D. Kirillov, E. I. Kuznetsov, S. V. Mirnov, M. P. Petrov, K. A. Razumova, V. S. Strelkov, and D. A. Shcheglov, Nucl. Fusion, Suppl., 17 (1968).

[14]G. A. Bobrovskiĭ, É. I. Kuznetsov, and K. A. Razumova, Zh. Eksp. Teor. Fiz. 59, 1103 (1970) [Sov. Phys.-JETP 32, 599 (1971)].

[15]F. L. Hinton and C. Oberman, Nucl. Fusion 9, 312 (1969).

[16]É. I. Kuznetsov, At. Énerg. 25, 315 (1968).

[17]S. V. Mirnov and I. B. Semenov, At. Énerg. 30, 20 (1971).

[18]Yu. N. Dnestrovskiĭ and D. P. Kostomarov, At. Énerg. 29, 434 (1970).

[19]A. A. Galeev and R. Z. Sagdeev, Zh. Eksp. Teor. Fiz. 53, 348 (1967) [Sov. Phys.-JETP 26, 233 (1968).

[20]V. L. Kazacha and Yu. S. Maksimov, Paper read at the Third All-union Conference on Plasma Diagnostics, Sukhumi, 1970.

[21]E. K. Zavoĭskiĭ and L. I. Rudakov, At. Énerg. 23, 417 (1967).

Translated by S. Chomet
227